INTERNATIONAL ATOMIC ENERGY AGENCY
UNITED NATIONS EDUCATIONAL, SCIENTIFIC AND CULTURAL ORGANIZATION

INTERNATIONAL CENTRE FOR THEORETICAL PHYSICS
34100 TRIESTE (ITALY) - P.O.B. 586 - MIRAMARE - STRADA COSTIERA 11 - TELEPHONES: 224281/2/3/4/5/6
CABLE: CENTRATOM - TELEX 460392-1

SMR/115 - 40

WINTER COLLEGE ON LASERS, ATOMIC AND MOLECULAR PHYSICS

(21 January - 22 March 1985)

MOLECULAR ELECTRONIC SPECTROSCOPY: AN INTRODUCTION

M.N.R. ASHFOLD
School of Chemistry
University of Bristol
Bristol BS8 1TS
U.K.

I INTRODUCTION

The electronic band spectra of diatomic molecules are prominent in the light emission from flames and discharges (Gaydon, 1974); the detailed analysis of the structure displayed in these spectra played an important role in the development of quantum theory. The spectra are characteristic not only of the molecular species which give rise to them, but also of the environment and mode of excitation. Thus they find many and varied applications including, for example,

(i) the study of rapid chemical reactions and of molecular photofragmentation processes, and

(ii) the identification of molecular species in the upper atmosphere, in planetary atmospheres and in comets. Spectral analysis can also provide information about the physical conditions prevailing in these varied environments.

Some polyatomic molecular spectra are observed in the emissions from flames and discharges, but most polyatomic species are chemically degraded in such sources. The electronic spectra of such species thus tend to have been studied in absorption and, more recently, through use of laser induced fluorescence and (in a few cases) multiphoton ionisation methods.

Formaldehyde was the first polyatomic molecule whose electronic spectrum succumbed to detailed spectroscopic analysis (Dieke and Kistiakowsky, 1934). The technique of flash photolysis, developed in the 1950's, led to the characterisation of many new electronic spectra associated with short-lived polyatomic species - most especially at the N. R. C. laboratories in Ottawa. The analysis of these spectra required the consolidation and extension of the theory of molecular spectroscopy. In the same period the electronic spectra of acetylene (Ingold and King,

1953), and later benzene (Callomon, Dunn and Mills, 1966) and ethylene (Merer and Mulliken, 1969) yielded to detailed analysis. Since the mid-1970's the laser induced fluorescence (LIF) technique has been responsible for another revolution in the study of molecular electronic spectroscopy: molecules (both neutrals and ions) and radicals have now been probed with a sensitivity, and at a resolution, that would have seemed unimaginable even a decade ago.

One feature that emerged from these analyses of polyatomic molecular spectra was the realisation that excited states could possess a molecular geometry and shape substantially different to that of the ground electronic state. Illustrative examples include: (i) C_2H_2, which has a linear ground state, but is trans- bent in the excited state that is responsible for it's near UV absorption bands, (ii) the HCO radical, which shows the converse behaviour, having a bent ground state but a linear first excited state and (iii) NH_3, which is pyramidal (C_{3v}) in its ground state but has a planar excited state geometry.

These lectures will begin with a brief review of the theory of the electronic states and spectra of diatomic molecules. This will be followed by a discussion of the corresponding topics for the case of polyatomic molecules. All examples cited in these sections refer to the gas phase, since it is only under these conditions that molecular rotation is unhindered and thus quantised. The 'spectroscopy' of continuum states will be considered also. The course will conclude with a summary of the photophysics and photochemistry of excited electronic states.

II DIATOMIC MOLECULES

The electronic states of a molecule will generally be much more widely separated in energy than the associated vibrational and rotational

level spacings. Thus it is normal to assume the Born-Oppenheimer separation of electronic and nuclear motion. For a diatomic molecule this leads to the following factorisation of the total wavefunction:

$$\Psi = \Psi_e(\underset{\sim}{r},R)\Psi_v(R)\Psi_r(\theta,\phi) \qquad (1)$$

where R is the internuclear separation, $\underset{\sim}{r}$ represents the set of electronic coordinates relative to the nuclei, and θ and ϕ are the rotational coordinates. Although Ψ_e varies parametrically with R, this dependence is usually weak and is often neglected.

II.1 Characterisation of Electronic States (Herzberg, 1950)

Within the Born-Oppenheimer separation each electronic state is characterised by a potential energy function U(R) which constrains the motion of the nuclei. For states with a potential minimum the quantised vibrational levels are the eigenvalues of the equation:

$$\left[-\frac{\hbar^2}{2\mu_{12}}\frac{d^2}{dR^2} + U(R)\right]\Psi_v(R) = E_v\Psi_v(R) \qquad (2)$$

where $\mu_{12} = m_1m_2/(m_1 + m_2)$ is the reduced mass of the two nuclei. The total electronic angular momentum associated with each Ψ_e is not defined (since the electronic potential is anisotropic) but the component along the internuclear axis is, and is given by $\Omega\hbar$. Ω is integral for molecules containing an even number of electrons, and half-integral for those with an odd number. For molecules composed of two light atoms, spin-orbit coupling is small. The electronic orbital and spin angular momenta are then independently quantised, with quantum numbers Λ (axial component

only), and S (total) and Σ (axial component) respectively. States are labelled by a term symbol of the form:

$$^{2S+1}\Lambda$$

in which the spin multiplicity 2S + 1 appears as a left superscript to the symbol representing the orbital angular momentum quantum number Λ (respectively Σ, Π, Δ,.... for Λ = 0, 1, 2,...). For Σ states it is necessary to add the symmetry to reflection in a plane containing the nuclei (Σ^+ or Σ^-). For homonuclear diatomics the symmetry to inversion of the electrons through the centre of symmetry must also be specified through use of the label g (gerade) for symmetric and u (ungerade) for antisymmetric states.

By far the strongest interaction between photons and molecules arises from the electric dipole moment operator $\underset{\sim}{\mu}$ and the electric vector ($\underset{\sim}{\epsilon}$) of the electromagnetic wave. Thus the overall transition probability depends on the square of the matrix element of the dipole operator $\left| \int \psi_e' \hat{\underset{\sim}{\mu}} \psi_e'' dr \right|^2$. Here, and throughout these notes, the upper state involved in a transition is denoted by a prime (ψ') and the lower state by a double prime (ψ''). For this matrix element to have a non-zero value the transition must obey the selection rules for allowed transitions:

$$\Delta\Lambda = 0, \pm 1 \qquad \Delta S = 0 \tag{3}$$

and, when appropriate

$$\left.\begin{array}{l} \Sigma^+ \longleftrightarrow \Sigma^+, \quad \Sigma^- \longleftrightarrow \Sigma^-, \quad \Sigma^+ \not\longleftrightarrow \Sigma^- \\ g \not\longleftrightarrow g, \quad u \not\longleftrightarrow u, \quad g \longleftrightarrow u \end{array}\right\} \tag{4}$$

Transitions which violate these rules are usually many orders of magnitude weaker than those which obey them, but transitions with $\Delta S \neq \pm 1$ do become increasingly intense with increasing atomic number as spin-orbit coupling weakens the validity of the S quantum number.

II.2 Molecular Orbitals

Comparison of the electronic states within related families of molecules (such as C_2, CN, N_2, NO, O_2) led to a realisation that, as in atoms, there existed an underlying pattern which could be described in terms of an aufbau (building up) principle. The ground state of each molecule is obtained from that of the preceding molecule by allocating the additional electron to a molecular orbital with integral axial quantum number λ. The Pauli Principle restricts the capacity of σ orbitals (λ=0) to 2 electrons; orbitals with λ>0 (e.g. π, δ orbitals) can contain up to 4 electrons. Filled shells give no contribution to Λ or S. Excited electronic states arise from the rearrangement of one or more electrons within the shells if the electronic configuration permits this, or promotion of one or more electrons from one orbital shell to another. For each such state the values of Λ and S are given by the vector addition of the values of λ_i and s_i for those electrons which are in non-filled shells.

The magnitude of the electronic transition probability is usually found to be large only when the electronic configuration of the two states involved differ by just a single electron for which $\Delta\lambda = 0, \pm 1$. Transitions which are allowed by the selection rules (3) and (4), but which involve double or more electron jumps, or single electron jumps for which $|\Delta\lambda| > 1$, usually have very small transition probabilities and behave like 'forbidden' transitions.

The molecular orbitals ϕ_i are eigenfunctions of an approximate electronic Hamiltonian, the Hartree-Fock operator $\hat{F}$:

$$\left.\begin{aligned} \hat{F}\phi_i &= \varepsilon_i(R)\phi_i \\ \text{where} \qquad \hat{F} &= -\frac{\hbar^2}{2m_e}\nabla^2 + V_{ne}(\underset{\sim}{r},R) + V_{eff}(\underset{\sim}{r}) \end{aligned}\right\} \qquad (5)$$

in which the potential of attraction to the nuclei, V_{ne}, is partially offset by an attractive potential V_{ee}^{eff} arising from the Coulomb and exchange repulsion between the electrons. These orbitals fall into three broad categories:

a) orbitals localised on one atomic centre, particularly inner shell orbitals, but also orbitals of the 'lone pair' type.

b) orbitals delocalised over the whole molecular framework, with either high electron density, or a nodal plane, in the region between the two nuclei.

c) Rydberg orbitals, which are much larger in mean radius than the internuclear separation.

Only molecular orbitals of type (b) contribute significantly to the bonding between two atoms, types (a) and (c) being essentially 'non-bonding'. Eqn. (5) may be solved most simply by constructing the ϕ_i from the atomic orbitals of the constituent atoms, taking one orbital for each set of atomic quantum numbers. This linear combination of atomic orbital (LCAO) approach gives a reasonable framework for understanding molecular spectra and bonding, even though it lacks quantitative accuracy. Figure 1 illustrates this approach for a homonuclear diatomic constructed from atoms in the first row of the periodic table.

Thus in the molecular orbital approach the changes in bonding occurring in an electronic transition are ascribed to the characters of the

vacated and newly occupied orbitals. In contrast, the transition energies cannot be simply equated to the difference between orbital energies ε_i because of the changes in electron repulsion resulting from changes in orbital occupation numbers.

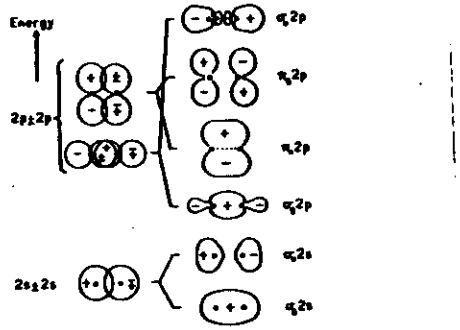

Fig.1 LCAO-molecular orbitals for homonuclear diatomic molecules. Only one of the two equivalent components of each π orbital is shown; the other components are perpendicular to the plane of the paper.

II.2 Vibrational Structure

A transition between two different electronic states of a diatomic molecule usually involves simultaneous changes in vibrational and rotational energy. By analysing such transitions, the equilibrium bond lengths and dissociation energies of the excited molecular states can sometimes be estimated. When studied at comparatively low resolution the spectra of diatomics are often observed to consist of a number of bands (c.f. the single line of an atomic transition). The frequencies of the bands arising from the transition v' - v" in each electronic transition may be expressed (in cm^{-1} units) as:

$$\nu = T_e + G'(v') - G''(v'') \qquad (6)$$

The electronic term T_e is the origin of the band system and corresponds to the energy separation between the minima of the potential energy curves of the electronic states coupled in the transition. The vibrational terms can usually be expressed as a rapidly convergent power series in v:

$$G(v) = \omega_e(v+\tfrac{1}{2}) - \omega_e x_e(v+\tfrac{1}{2})^2 + \omega_e y_e(v+\tfrac{1}{2})^3 - \ldots \qquad (7)$$

The vibrational level spacings decrease to zero at the dissociation limit. The extent of the vibrational structure observed in association with an electronic transition depends both on the temperature, and thus the range of populated levels, and also on the nature of the combining states.

Precisely which vibrational levels are coupled in an electronic transition is determined by the Franck-Condon Principle. Individual

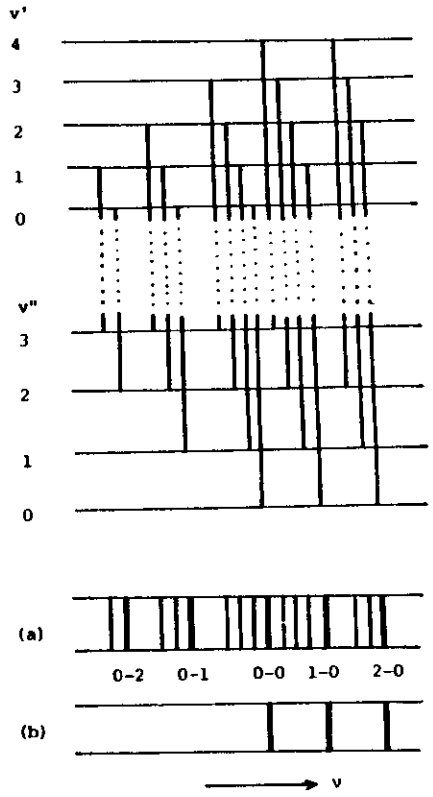

Fig.2 The vibrational structure of an electronic band system of a diatomic molecule, (a) in emission at high temperature, (b) in absorption at low temperature.

v' - v" transition probabilities may be evaluated using the Born-Oppenheimer wavefunction of eqn.(1). These take the form:

$$\left[\int \psi_v'^*(R)\left[\int \psi_e'^*(\underset{\sim}{r},R)\,\underset{\sim}{\mu}\,\psi_e''(\underset{\sim}{r},R)\,d\tau_e\right]\psi_v''(R)\,d\tau_v\right]^2 \qquad (8)$$

If the electronic transition moment varies only slowly, or not at all, with R this integral may be factorised to:

$$\left[\int \psi_{v'} {}^{*} \psi_{v''} d\tau_{v}\right]^{2} \cdot \left[\int \psi_{e'} {}^{*} \underset{\sim}{\mu} \psi_{e''} d\tau_{e}\right]^{2} \qquad (9)$$

The relative intensities of the vibrational bands are thus determined by the vibrational overlap integral, or Franck-Condon factor:

$$q_{v'v''} = \left[\int \psi_{v'} {}^{*} \psi_{v''} d\tau_{v}\right]^{2} \qquad (10)$$

When these factors are summed over all final states for a given initial state the result is unity. Thus in this approximation the integrated intensity of absorption is independent of the initial state.

The physical interpretation of the Franck-Condon factor goes back to the original basis of the Born-Oppenheimer separation, namely that nuclei are (relatively) so massive in comparison with electrons that they may be considered as being stationary over the timescale of an electronic transition. Thus on potential energy curve diagrams such as those shown in fig.3 the molecule must execute a 'vertical' transition, such that it is prepared in the excited electronic state with the same internuclear separation as it had in the ground electronic state. Thus, the only regions of the excited state potential that are accessible in absorption are those for which the vibrational wavefunction of the ground state has finite amplitude. Analagous arguments hold for emission spectra, as demonstrated schematically in fig.3. If the vibrational wavefunctions have several nodes, there will be interference between the two, leading to irregular variations in the Franck-Condon factors.

For electronic transitions which result in only small changes in internuclear separation R_e and vibrational frequency ω_e, the vibrational intensity distribution is controlled largely by the change, ΔR_e, in the internuclear separation. Franck-Condon factors calculated using a

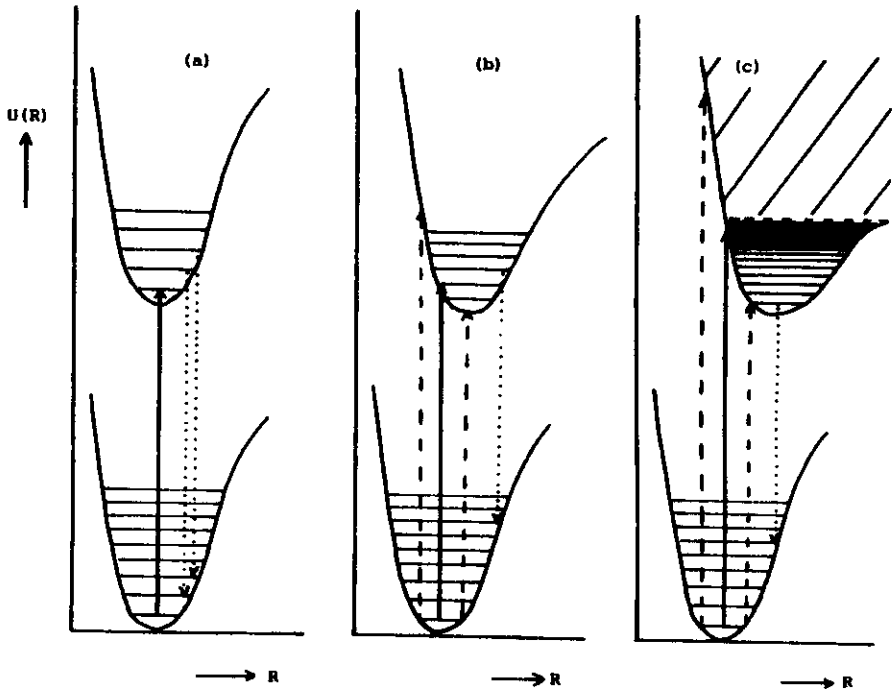

Fig.3 Vertical transitions in electronic band systems between states with (a) very similar, (b) slightly different, (c) very different potential curves. Included also are the strongest band (⟶) and the first and last (- - -▸) bands in absorption, and the strongest emission band (·····▸) from a given v' level.

harmonic approximation can then be fitted to the observed intensity distribution, leading to a determination of ΔR_e. Fig.4 illustrates how the intensity distribution along a v' - 0 absorption progression depends on ΔR_e. The dimensionless variable δ is the ratio of ΔR_e to the classical zero-point amplitude s_0 given by:

$$s_0 = \left[\frac{h}{4\pi^2 c \mu_{12} \omega}\right]^{\frac{1}{2}} \qquad (11)$$

or
$$s_0/\text{nm} = \frac{0.5807}{\left[(\mu_{12}/\text{amu})\,(\omega/\text{cm}^{-1})\right]^{\frac{1}{2}}} \qquad (12)$$

The Franck-Condon factors in this model are given by:

$$q_{v'-0} = (\tfrac{1}{2}\delta^2)^v \exp(-\tfrac{1}{2}\delta^2)/v! \qquad (13)$$

Such a quantitative application of the Franck-Condon principle is particularly useful if it is not possible to determine R_e from a rotational analysis.

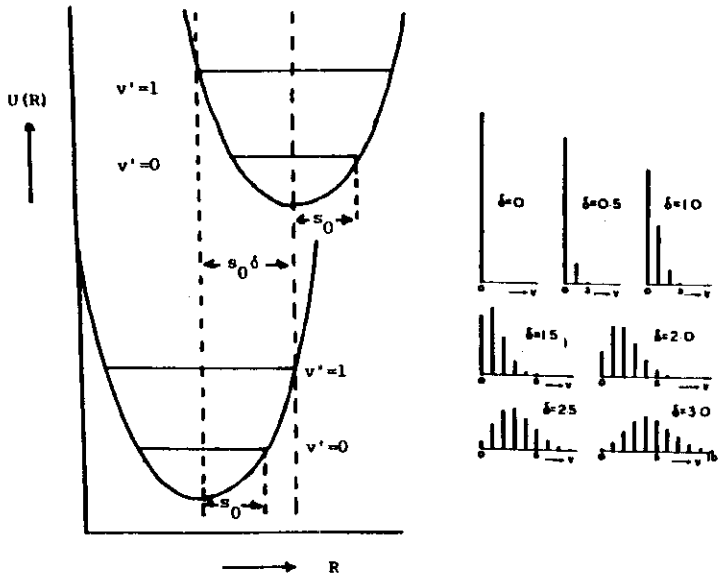

Fig.4 The variation in intensity along a v'-0 absorption progression as given by Franck-Condon factors $q_{v'v''}$. The factors are calculated assuming harmonic vibrations with $\omega' = \omega''$, but with various ratios δ of the change in ΔR_e in equilibrium bond length to the vibrational amplitude s_0 for v"=0.

II.4 Rotational Structure

When viewed under higher resolution, each of the bands contributing to the vibrational structure of an electronic transition is seen to be composed of a large number of discrete lines. These are due to the various possible rotational energy changes that accompany each v'-v" transition. The rotational selection rules depend on the molecule-fixed component of the dipole operator that renders the transition allowed. This lies parallel to the internuclear axis for $\Delta\Lambda=0$ transitions, but perpendicular to the axis for $\Delta\Lambda=\pm1$. In each vibrational state of a singlet electronic state the rotational term values are, neglecting centrifugal distortion, given by;

$$F(J) = B_v\left[J(J+1)-\Lambda^2\right] \qquad (14)$$

where the rotational constant B_v is proportional to the average inverse of the moment of inertia:

$$B_v = \frac{h}{8\pi^2 c}\left\langle\frac{1}{I}\right\rangle$$

or
$$B_v/\text{cm}^{-1} = \frac{16.8575}{\mu_{12}/\text{amu}} \cdot \left\langle\frac{1}{(R/\text{Å})^2}\right\rangle \qquad (15)$$

In general there are three possible branches with line frequencies given by:

$$\Delta J=-1 \quad \text{(P branch)} \quad \nu = \nu_o - (B'+B'')J + (B'-B'')J^2$$

$$\Delta J=0 \quad \text{(Q branch)} \quad \nu=\nu_o+(B'-B'')J^2$$
$$\Delta J=+1 \quad \text{(R branch)} \quad \nu=\nu_o+(B'+B'')(J+1)+(B'-B'')(J+1)^2 \qquad (16)$$

In these equations J is the rotational quantum number J" for the lower state, and in each state $J \geq \Lambda$. Thus if $\Lambda>0$ there will be "missing lines" close to the band origin ν_o, from which the value of Λ can be deduced. The branch intensity rules are:

$^1\Sigma-^1\Sigma$ $(\Delta\Lambda=0)$

P and R branches only

$^1\Pi-^1\Pi$ $(\Delta\Lambda=0$, but $\Lambda>0)$

There is also a weak Q branch

$^1\Delta-^1\Pi$ $(\Delta\Lambda=\pm1)$

Q branch twice as strong as the P and R branches

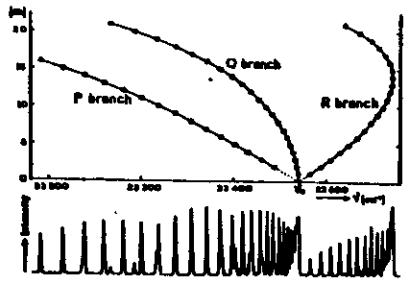

Fig.5 The three branches of the 424.1nm band of AlH($^1\Pi - {}^1\Sigma^+$).

Fig. 5 plots the line frequencies of a band of AlH against a running number m which is -J for the P branch, J for the Q branch and (J+1) for the R branch. In this example B' is about 5% smaller than B", leading to the formation of a band head in the R branch and strongly degraded P and Q branches.

For states with S>0 the magnetic moment of the electron spins will interact with the magnetic field of the orbital and rotational motions. The splitting between the resultant (2S+1) multiplet components varies greatly from one molecule to another: as in atoms it tends to increase with atomic number.

The rotational constant for the v=0 level of an electronic state can lead through equ. (15) to a reasonable estimate of the equilibrium bond length R_e. Data from a number of vibrational levels can lead not only to an extrapolation to give the true R_e, but also to the complete potential curve U(R). Additionally, it should be clear that rotational analyses provide one clear cut route to establishing the symmetry of excited electronic states.

III POLYATOMIC MOLECULES

The electronic spectra of polyatomic molecules (Herzberg, 1966) are more complicated than those of diatomic molecules for a number of reasons, including:

(i) there is a wider range of types of molecular orbital because of the presence of many atomic centres, with the possibility of changes in shape when electrons are excited;

(ii) an N-atom molecule has 3N-6 (or 3N-5 if linear) vibrational degrees of freedom, and several of these may be simultaneously

excited; and

(iii) non-linear molecules have three rotational degrees of freedom, giving many more rotational branches in a single vibronic band.

III.1 Vibrational Structure

The vibrational term values in an electronic state of a polyatomic molecule require a quantum number for each mode of vibration: the extension of eqn. (7) is:

$$G(v_1,v_2,\ldots) = \sum_i \omega_i\left(v_i+\frac{d_i}{2}\right)+\sum_i\sum_{k>i} x_{ik}\left(v_i+\frac{d_i}{2}\right)\left(v_k+\frac{d_k}{2}\right)\ldots \qquad (17)$$

where v_i, v_k are the vibrational quantum numbers, ω_i are the vibrational frequencies and the x_{ik} are anharmonicity constants. Note that the anharmonicity constants are defined in a manner different from that of the diatomic case. The degeneracy factors d_i allow for the cases where two or more vibrations have the same frequency because of some high symmetry in the molecule.

The red and near infrared absorption spectra of the bent triatomic radicals HNO and DNO provide an illustrative example. Vibrational bands observed in the HNO spectrum have frequencies given by:

$$\begin{aligned}\nu\ /\mathrm{cm}^{-1} = 13154.4 &+ 2854.2v_1' + 1445.1v_2' + 981.2v_3' - 7.3v_1'v_2' \\ &-19.2v_1'v_3' - 26.5v_2'^2 - 12.9v_2'v_3' - 5.4v_1'v_2'v_3' \\ &+ 2.2v_2'^3 \qquad (18)\end{aligned}$$

whilst those in DNO fit the formula:

$$\begin{aligned}\nu\ /\mathrm{cm}^{-1} = 13180.3 &+ 2176.5v_1' + 1419.5v_2' + 755.3v_3' - 24.9v_1'v_2' \\ &+ 2.3v_1'v_3' - 18.2v_2'^2 - 61.5v_2'v_3' + 21.6v_2'^2v_3' \qquad (19)\end{aligned}$$

Thus all three vibrational modes are active in these band systems. Note how isotopic substitution can aid assignment of these modes; ω_2' is almost invariant to deuteration and can thus be identified with a mode which is predominantly N-O stretching.

In contrast, the bent triatomic radicals HCF and HCCl both have visible band systems with a long progression of bands, but these correspond to excitation of only one mode of vibration.

The Franck-Condon principle can account for such differences. Only those vibrational modes which distort the ground state structure towards the equilibrium geometry of the excited electronic state will be strongly excited with large Δv. In both HCF and HCCl rotational analyses reveal that there is a substantial ($\sim 30^\circ$) change in bond angle upon excitation, but almost no change in the bond lengths. Consequently only the bending vibration is strongly active in their respective visible electronic spectra. However in those instances where electronic excitation is accompanied by a significant change in (at least) one bond length, bands involving the appropriate stretching vibration(s) will appear also. Provided that changes in geometry are not too large and that, therefore, the forms of the upper and lower state normal vibrations are similar, the Franck-Condon factor (eqn.10) may be expressed as a product of terms, one for each normal mode:

$$q_{v_1'v_2'\ldots,v_1''v_2''\ldots} = \left[\int \psi_{v_1'}^{*}\psi_{v_1''}d\tau_1\right]^2\left[\int \psi_{v_2'}^{*}\psi_{v_2''}d\tau_2\right]^2\ldots \qquad (20)$$

Figure 6 shows how the intensity distribution is built up when two modes are excited, one (v_1) more strongly than the other (v_2). Each band

in the progression $v_1 0\text{-}00$ marks the beginning of a progression in v_2, and each of these has the same relative intensity distribution.

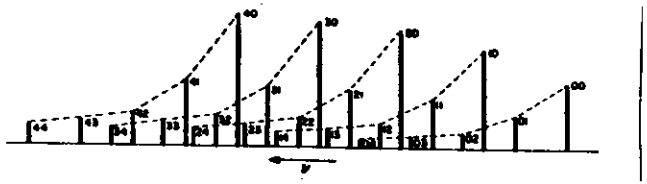

Fig.6 Schematic low temperature absorption spectrum showing progressions in two upper state vibrations. The numbers attached to the various bands are the $v_1'v_2'$ values. All bands have $v_1'' = v_2'' = 0$.

III.3 Vibrational Selection Rules

HNO, HCP and HCCl are all bent triatomic radicals; as such they belong to the C_s point group and all their modes of vibration are totally symmetric (a'). In molecules of higher symmetry some of the vibrational modes are antisymmetric to at least one symmetry element. Herzberg and Teller (1933) derived the following vibrational selection rules by considering the symmetry properties of the Franck-Condon overlap integral:

(i) Vibrations which are totally symmetric with respect to all of the symmetry operations of the molecular point group may change by any number of quanta.

(ii) Vibrations which are antisymmetric with respect to at least one symmetry operation may change only by $\Delta v = 0, \pm 2, \pm 4, \ldots$

In the latter case the transitions with $\Delta v = 0$ are very much stronger than those with $\Delta v \neq 0$. For this reason the asymmetric stretching

vibration ν_3 is known for the excited states of very few AH_2 or AB_2 molecules, whether these are linear or bent.

When applying these rules to a molecule that undergoes a shape change upon electronic excitation only the symmetry operations common to both point groups must be considered. Fig.7 illustrates the vibrational state changes that accompany the near UV electronic absorption of NH_3, which have band frequencies given by:

$$\nu\ /\mathrm{cm}^{-1} = 46136 + 874v_2' + 4.0v_2'^2 \qquad (21)$$

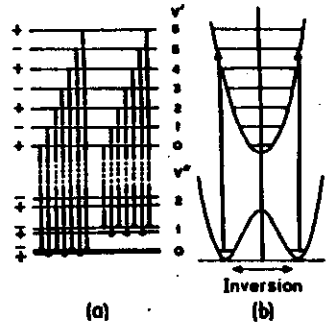

Fig.7 (a) The vibrational transitions for a planar - non-planar electronic transition, indicating the origin of 'staggering' in progressions in absorption. (b) The vertical transitions from the lowest vibrational level of NH_3.

Ammonia is pyramidal (C_{3v}) in its electronic ground state, but planar (D_{3h}) in its excited $\tilde{A}$ state. The frequency $874cm^{-1}$ is associated with the excited state out-of-plane bending vibration. This mode is symmetric (a_1) in C_{3v}, but antisymmetric with respect to the molecular plane in D_{3h}. The long vibrational progression has a maximum at $v_2' \sim 7$ in NH_3, and a Franck-Condon analysis quantitatively confirms the pyramidal to planar transition. The influence of symmetry to this plane becomes apparent when analysing the progression of hot band absorptions involving $v_2'' = 1$. This level in the ground electronic state has a substantial splitting ($\sim 36cm^{-1}$) due to tunnelling through the barrier to inversion; this leads to an alternating spacing in the progression of hot bands.

III.3 Rotational Structure

The rotational energy levels of a non-linear polyatomic molecule can be expressed in terms of the three principal moments of inertia I_A, I_B, and I_C ($I_A \leq I_B \leq I_C$ by convention). If these three moments are all different the molecule is an asymmetric top. If two moments are equal it is a symmetric top. Linear molecules are the limiting case of symmetric top molecules having $I_A = 0$ and $I_B = I_C$.

For linear molecules the rotational energy levels are given by an expression similar to eqn.(14):

$$F(J,K) = B_v\left[J(J+1) - K^2\right] - D_v\left[J(J+1) - K^2\right]^2 \ldots \qquad (22)$$

in which the variation of the moment of inertia with rotation (centrifugal distortion) has been incorporated through inclusion of the small correction with constant D_v. As before, J is the quantum number for the total

angular momentum and K that for its component along the internuclear axis; this can arise from both electronic and bending vibrational motion. Thus $J \geq K$.

For symmetric top molecules there are two distinct rotational constants and three centrifugal distortion constants. For a prolate ($I_A < I_B = I_C$) symmetric top the equation for the rotational term values is:

$$F(J,K) = AK^2 + B\left[J(J+1) - K^2\right] - D_K K^4 - D_{JK} J(J+1) K^2 - D_J J^2 (J+1)^2 \qquad (23)$$

The corresponding equation for an oblate symmetric top has the same form and is obtained by replacing A in eqn.(23) by C.

For an asymmetric top molecule there exists no such closed-form expression for the (2J+1) rotational energy levels associated with each J value. However, in many small molecules (e.g. ethylene, formaldehyde) and radicals (e.g. HCO, HNO) B and C are nearly equal, and eqn.(23) with $\bar{B} = \frac{1}{2}(B+C)$ substituted in place of B provides a good first approximation to the rotational energies. When this approach is inadequate it is now usual to compute energy levels using trial rotational constants by diagonalising matrices of the rotational hamiltonian using a fast computer, and thereby fitting experimental data numerically. A quantitative measure of the departure from the limiting symmetric top cases is provided by the asymmetry parameter κ:

$$\kappa = \frac{2B-A-C}{A-C} \qquad (24)$$

which takes values between the prolate limit ($\kappa=-1$) and the oblate limit ($\kappa=+1$).

There may be other additions to eqn.(23) as a result of spin multiplet splittings, vibrational angular momentum or higher order centrifugal distortion corrections.

Linear polyatomic molecules are subject to the same rotational selection rules as diatomics, i.e.

$$\begin{array}{lll} \text{If } \Delta K = 0 & \Delta J = 0, \pm 1 & (\text{but } \Delta J = \pm 1 \text{ only for } K = 0) \\ \Delta K = \pm 1 & \Delta J = 0, \pm 1 & \end{array} \qquad (25)$$

Since each vibrational level is associated with a different value of K each band will be of parallel (weak or absent Q branch) or perpendicular (strong Q branch) character. Each vibration of a linear molecule is itself either parallel (σ) or perpendicular (π). The latter type is not totally symmetric; the Herzberg-Teller rules thus indicate that vibrations of this type of band should not be active in odd quanta. Thus the bands in one band system should all exhibit parallel rotational structure or all show perpendicular rotational structure, depending on the value of $\Delta\Lambda$. In practice it is usual to find that all the strong bands in a given spectrum are of the same type, but exceptions can arise due to vibronic interaction (see later).

In a symmetric top molecule K is a good quantum number; hence one vibrational state may possess many K values. Each band of a symmetric top molecule is thus more complicated than a band of a diatomic molecule, since there are P, Q and R branches for each populated value of K. Bands are of two general types:

(a) transition moment parallel to the top axis (parallel band)

$$\begin{array}{lll} \Delta K = 0, & \Delta J = \pm 1 & \text{if } K = 0 \\ & \Delta J = 0, \pm 1 & \text{if } K > 0 \end{array} \qquad (26)$$

The branches are labelled ${}^{Q}P$, ${}^{Q}Q$ and ${}^{Q}R$, where the left superscript represents ΔK.

(b) transition moment perpendicular to the top axis (perpendicular band)

$$\Delta K = \pm 1, \quad \Delta J = 0, \pm 1 \qquad (27)$$

with branches labelled ${}^{P}P$, ${}^{P}Q$, ${}^{P}R$, ${}^{R}P$, ${}^{R}Q$ and ${}^{R}R$.

There is no good K quantum number in a strongly asymmetric top molecule; the rotational selection rules are correspondingly more relaxed. The only strict selection rules are:

$$\Delta J = 0, \pm 1 \qquad (28)$$

and

$$+ \leftrightarrow + \qquad - \leftrightarrow - \qquad + \leftrightarrow - \qquad (29)$$

each level having a well defined parity to inversion of all the particles in the molecule through its centre of mass. Each level may be further designated by the values of K_a and K_c of the symmetric top K quantum number with which the level correlates in the prolate and oblate limits respectively. This leads to the notation

$$J_{K_a,K_c} \qquad (30)$$

Each band may have its transition moment parallel to the a-, b- or c- inertial axis; the corresponding selection rules are :

$$\left.\begin{array}{llll} \text{(i)} \quad \text{type a band} & \Delta J = 0, \pm 1, & \Delta K_a = \text{even}, & \Delta K_c = \text{odd} \\ \text{(ii)} \quad \text{type b band} & \Delta J = 0, \pm 1, & \Delta K_a = \text{odd}, & \Delta K_c = \text{odd} \\ \text{(iii)} \quad \text{type c band} & \Delta J = 0, \pm 1, & \Delta K_a = \text{odd}, & \Delta K_c = \text{even} \end{array}\right\} \qquad (31)$$

In some molecules of low symmetry the transition moment may not be confined to lie along one of the principal inertial axes; in such cases a hybrid band results.

III.4 Vibronic Interaction

The Herzberg-Teller rules predict that all the bands in a given band system will be of the same type - determined by the symmetry of the electronic transition moment $\int \Psi_e' {}^* \mu \Psi_e'' d\tau_e$. There are, however, many exceptions to this. The blue $^2\Sigma^+ - {}^2\Pi$ band system of NCO provides one example. As expected all the strong bands in this system are perpendicular bands, but a number of weaker bands involving $\Delta v_2 = \pm 1$ appear also, (v_2 being the bending vibrational quantum number). These weak bands violate the Herzberg-Teller rules, but they are not symmetry forbidden. The overall symmetry of the vibronic wavefunction Ψ_{ev} is given by the direct product of that for the two component wavefunctions:

$$\Gamma(\Psi_{ev}) = \Gamma(\Psi_e) \times \Gamma(\Psi_v) \qquad (32)$$

In the case of NCO we have:

$^2\Pi$ state:	$v_2'' = 0$	$\Gamma(\Psi_v) = \sigma^+$	$\Gamma(\Psi_{ev}) = {}^2\Pi$
	$v_2'' = 1$	$\Gamma(\Psi_v) = \pi$	$\Gamma(\Psi_{ev}) = {}^2\Sigma^+ + {}^2\Sigma^- + {}^2\Delta$
$^2\Sigma^+$ state	$v_2' = 0$	$\Gamma(\Psi_v) = \sigma^+$	$\Gamma(\Psi_{ev}) = {}^2\Sigma^+$
	$v_2' = 1$	$\Gamma(\Psi_v) = \pi$	$\Gamma(\Psi_{ev}) = {}^2\Pi$

Thus there is a (1,0) band which corresponds to a $^2\Pi - {}^2\Pi$ transition, and a (0,1) band which is $^2\Sigma^+ - {}^2\Sigma^+$. The intensity of these bands arises from the variation of Ψ_e with the bending coordinate - a variation which is neglected in the formulation of the Franck-Condon principle (eqns.8-10):

$$\Psi_e(q_1, \ldots q_n) = \Psi_e(0) + \sum_i \left(\frac{d\Psi_e}{dq_i}\right)_0 q_i \ \ldots\ldots \qquad (33)$$

As a result of this vibrational - electronic (vibronic) interaction the transition moment is also a function of the vibrational coordinates q_i, whatever their symmetry. In a perturbation theory approach this variation is ascribed to the mixing of electronic states when the molecule is deformed from its equilibrium geometry, and the resultant band intensity is 'borrowed' from a symmetry allowed band system.

The near UV band system of H_2CO represents one important example of vibronic interaction. It involves an electric dipole forbidden $^1A_2 - {}^1A_1 (C_{2v})$ electronic transition and arises principally through excitation of the symmetry-lowering out of plane bending vibration $\nu_4(b_1)$, which leads to the symmetry allowed vibronic transitions shown in Table 2.

Table 2

The species of the vibronic levels of the $^1A_2$ and $^1A_1$ states of formaldehyde with excitation of the out-of-plane vibration. The vibrational quantum numbers are those for a planar molecule

Level		Electronic	Vibrational	Vibronic	Allowed electric dipole transitions
Upper state	v_4 odd	$^1A_2$	B_1	$^1B_2$	←
	v_4 even	$^1A_2$	A_1	$^1A_2$	←
Lower state	v_4 odd	$^1A_1$	B_1	$^1B_1$	←
	v_4 even	$^1A_1$	A_1	$^1A_1$	←

In molecular orbital terms this transition corresponds to the excitation of an electron from the b_2 non-bonding orbital localised on the oxygen atom to the b_1 antibonding π^* orbital. The out of plane vibration

leads to mixing between σ and π molecular orbitals (i.e. change of hybridisation at the carbon atom) (see fig.8). The π^* - n transition may be envisaged to have borrowed intensity from the symmetry allowed σ^* - n transition to shorter wavelengths. For this transition the dipole moment is parallel to the y axis (B_2).

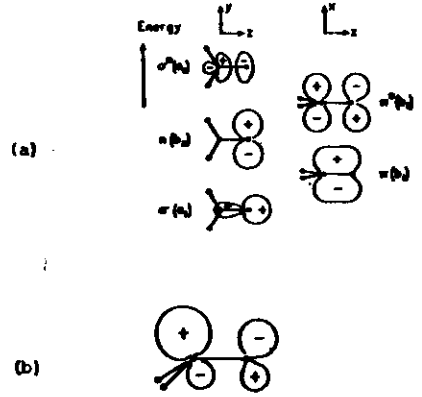

Fig.8 (a) Schematic representations of the highest occupied and lowest unoccupied molecular orbitals of formaldehyde.
(b) demonstrates the effect of an out-of-plane deformation of the π^* orbital.

The near UV band system of benzene is also symmetry forbidden, being $^1B_{2u} - {}^1A_{1g}(D_{6h})$. Fig.9 demonstrates that one consequence of the vibronic interaction which induces this transition is that the apparent origin of the absorption band has a different frequency from that of the fluorescence spectrum.

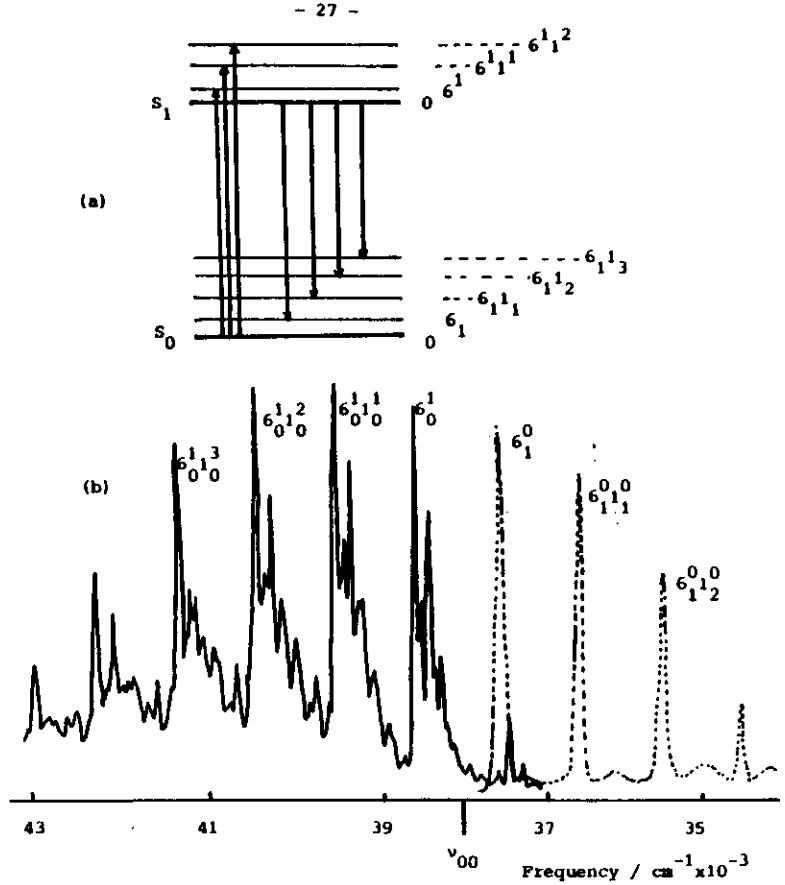

Fig.9 Absorption (——) and fluorescence (·····) of benzene vapour. (a) The main features in the vapour absorption spectrum and the fluorescence from the zero-point level of the S_1 state under isolated molecule conditions shown in (b). The 0 - 0 transition is absent because of symmetry restrictions.

IV MOLECULAR ORBITAL DIAGRAMS

As in diatomics, the change in bonding that accompanies electronic excitation in a polyatomic molecule may be ascribed to the properties of the donor and acceptor molecular orbitals. Walsh (1953) considered the variation of the orbital energies in simple molecules with changes in the interbond angles. The resulting theory has been most successful in predicting the characteristics of the spectra of polyatomic molecules.

IV.1 AH_2 molecules

The lowest energy molecular orbitals for AH_2 molecules may be formed by overlapping the s- and p- atomic orbitals in the valence shell of the A atom with the 1s orbitals of the H atoms. Consider the two limiting cases of (a) a linear AH_2 molecule and (b) a bent AB_2 molecule with $\hat{HAH} = 90^\circ$ (see fig.10).

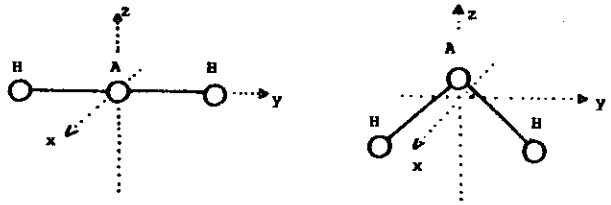

Fig.10

It is convenient to consider the orbitals of the two H atoms as a group, the two possible group orbitals being formed by the (1s+1s) in phase addition and the (1s-1s) out of phase addition of the two 1s atomic orbitals. In addition, for the bent (90°) AH_2 molecule, it is convenient to replace the p- orbitals of A which initially may be considered to lie along the A - H bond directions, by two

equivalent orbitals p_y and p_z lying parallel to the y- and z-directions respectively. Table 3 lists the components from which the molecular orbitals can be constructed and their symmetries.

Table 3

Linear molecule		Bent molecule	
A atom	H_2 group	B atom	H_2 group
s_A, σ_g p_y, σ_u p_x,p_z, π_u	(1s+1s), σ_g (1s-1s), σ_u	s_A, a_1 p_z, a_1 p_y, b_2 p_x, b_1	(1s+1s), a_1 (1s-1s), b_2

Only components of the same symmetry may mix to form molecular orbitals. For the linear molecule the procedure is straightforward. For the bent molecule Walsh introduced an assumption, namely that the geometry is determined by the directional properties of the p- valencies on the A atom and that the s_A- orbital does not mix with the other orbitals of a_1 symmetry. Table 4 lists the molecular orbitals for linear and bent (90°) AB_2, and shows the correlation between the two limiting configurations.

It now remains to decide the energetic ordering of the various orbitals and the variation in the energy of a particular orbital with valence angle. Estimates of the relative binding energies are based on the principles (i) that s- electrons are more tightly bound than p- electrons, and (ii) that the binding energy

Table 4

Linear molecule		Bent molecule
s_A + (1s+1s), σ_g	⟶	p_z + (1s+1s), a_1
p_y + (1s-1s), σ_u	⟶	p_y + (1s-1s), b_2
p_x, p_z, π_u	⟶	s_A, a_1 ; p_x, b_1
s_A - (1s+1s), $\bar{\sigma}_g$	⟶	p_z - (1s+1s), $\bar{a}_1$
p_y - (1s-1s), $\bar{\sigma}_u$	⟶	p_y - (1s-1s), $\bar{b}_2$

increases with increasing overlap of the component orbitals. These considerations indicate that the ordering given in Table 4 will approximate the order of decreasing binding energy downwards. The last two orbitals in each configuration are antibonding orbitals - distinguished by the inclusion of a bar over the symbol for the orbital.

Walsh identified two factors of importance when considering the variation of binding with valence angle. Firstly, an orbital becomes more tightly bound with change of angle if it changes from being built from a p- orbital of A to being built from an s- orbital of A. Secondly, orbitals that are antibonding between the end atoms are most tightly bound when those atoms are as far apart as possible (i.e. in the linear molecule). This second effect is generally subsiduary to the former. Thus we arrive at the predictions listed in Table 5.

Table 5

Molecular orbital	Variation in binding energy with decrease of angle	
Linear - Bent	First effect	Second effect
σ_g - a_1	Decrease	Increase
σ_u - b_2	No change	Decrease
π_u - a_1	Increase	No change
π_u - b_1	No change	No change
$\bar{\sigma}_g$ - $\bar{a}_1$	Decrease	Increase
$\bar{\sigma}_u$ - $\bar{b}_2$	No change	Decrease

The Walsh diagram for an AH_2 molecule, constructed on the basis of these principles, is shown in fig.11. The antibonding orbitals correlate with Rydberg orbitals (Mulliken, 1976) and lie at fairly high energies.

IV.2 HAB, AB_2 and ABC molecules

Walsh (1953) used the same approach when constructing orbital diagrams for molecules of the type HAB, AB_2 and ABC. In these cases the overlap of p- orbitals on the A and B atoms can lead to bonding and antibonding π molecular orbitals as well as σ orbitals and non-bonding orbitals. Representative Walsh diagrams

are displayed in figs.12 and 13, whilst Tables 7 and 8 demonstrate how well the experimental data accords with these predictions.

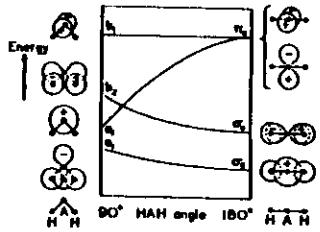

Fig.11 Walsh diagram for the four lowest intravalency shell orbitals of an AH_2 molecule and their approximate descriptions.

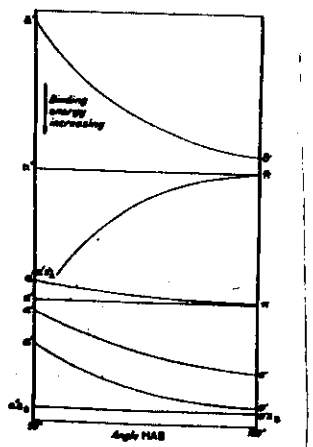

Fig.12

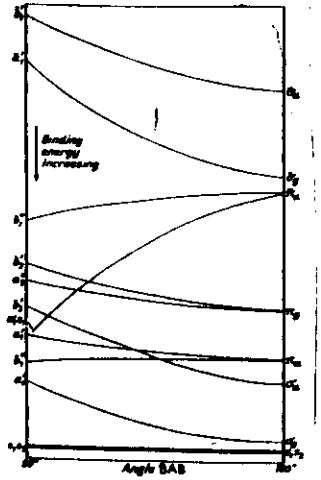

Fig.13

Table 6

Molecular orbitals and gemetries for AH_2 molecules [a]

		$a_1-\sigma_g$	$b_2-\sigma_u$	$sa_1-\pi_u$	$b_1-\pi_u$	$\hat{HAH}^\circ$	r_o(AH)
BeH_2	$\tilde{X}^1\Sigma_g^+$	2	2			180[b]	
BH_2	$\tilde{X}^2A_1$	2	2	1		131	1.18
	$\tilde{A}^2B_1$ (Π)	2	2		1	180	1.17
CH_2	$\tilde{X}^3B_1$	2	2	1	1	136	1.08
	$\tilde{a}^1A_1$	2	2	2		102	1.11
	$\tilde{b}^1B_1$	2	2	1	1	140	1.06
NH_2	$\tilde{X}^2B_1$	2	2	2	1	103	1.02
	$\tilde{A}^2A_1$ (Π)	2	2	1	2	144	1.00
H_2O^+	$\tilde{X}^2B_1$	2	2	2	1	111	1.00
H_2O	$\tilde{X}^1A_1$	2	2	2	2	105	0.96
SiH_2	$\tilde{X}^1A_1$	2	2	2		92	1.51
	$\tilde{A}^1B_1$ (Π)	2	2	1	1	123	1.49
PH_2	$\tilde{X}^2B_1$	2	2	2	1	92	1.42
	$\tilde{A}^2A_1$ (Π)	2	2	1	2	123	1.39
H_2S^+	$\tilde{X}^2B_1$	2	2	2	1	93	1.36
	$\tilde{A}^2A_1$ (Π)	2	2	1	2	127	1.37
H_2S	$\tilde{X}^1A_1$	2	2	2	2	92	1.33

a From Duxbury (1975)

b Predicted

Table 7

Molecular orbitals and geometries for HAB molecules [a]

		σ a'	σ a'	σ a'	π a"	π a'	π̄ a'	π̄ a"	r_o(AH)	r_o(AB)	ĤAB°
HCN	$\tilde{X}^1\Sigma^+$	2	2	2	2	2			1.06	1.16	180
	$\tilde{A}^1A''$	2	2	2	1	2	1		1.14	1.30	125
HCP	$\tilde{X}^1\Sigma^+$	2	2	2	2	2			1.07	1.54	180
	$\tilde{A}^1A''$	2	2	2	1	2	1		(1.14)	1.69	128
HCO	$\tilde{X}^2A'$	2	2	2	2	2	1		1.13	1.18	125
	$\tilde{A}^2A''(\Pi)$	2	2	2	2	2		1	1.06	1.19	180
HNO	$\tilde{X}^1A'$	2	2	2	2	2	2		1.06	1.21	109
	$\tilde{A}^1A''$	2	2	2	2	2	1	1	1.04	1.24	116
HPO	$\tilde{X}^1A'$	2	2	2	2	2	2		(1.43)	1.51	105
HCF	$\tilde{X}^1A'$	2	2	2	2	2	2		(1.12)	1.31	102
	$\tilde{A}^1A''$	2	2	2	2	2	1	1	(1.12)	1.30	127
HCCl	$\tilde{X}^1A'$	2	2	2	2	2	2		1.12	1.69	103
	$\tilde{A}^1A''$	2	2	2	2	2	1	1			134
HSiCl	$\tilde{X}^1A'$	2	2	2	2	2	2		1.56	2.06	103
	$\tilde{A}^1A''$	2	2	2	2	2	1	1	1.50	2.05	116
HNF	$\tilde{X}^2A''$	2	2	2	2	2	2	1	(1.06)	1.37	105
	$\tilde{A}^2A'$	2	2	2	2	2	1	2	(1.03)	1.34	125

a From Duxbury (1975)

Numbers in brackets denote assumed values.

Table 8

Molecular orbitals and geometries for AB_2 molecules.[a]

		σ_g a_1	π_u b_1 a_1	σ_u b_2	π_g a_2 b_2	π_u a_1 b_1	r_o(AB)	ĤAB°
C_3	$\tilde{X}^1\Sigma_g^+$	2	4	2			1.277	180
	$\tilde{A}^1\Pi_u$	2	4	1	1		1.305	180
CNC	$\tilde{X}^2\Pi_g$	2	4	2	1		1.245	180
	$\tilde{A}^2\Delta_u$	2	4	1	2		1.249	180
	$\tilde{B}^2\Sigma_u^-$	2	4	1	2		1.259	180
NCN	$\tilde{X}^3\Sigma_g^-$	2	4	2	2		1.232	180
	$\tilde{A}^3\Pi_u$	2	4	1	3		1.233	180
BO_2	$\tilde{X}^2\Pi_g$	2	4	2	3		1.265	180
	$\tilde{A}^2\Pi_u$	2	3	2	4		1.302	180
	$\tilde{B}^2\Sigma_u^+$	2	4	1	4		1.273	180
N_3	$\tilde{X}^2\Pi_g$	2	4	2	3		1.181	180
	$\tilde{B}^2\Sigma_u^+$	2	4	1	4		1.180	180
CO_2^+	$\tilde{X}^2\Pi_g$	2	4	2	3		1.177	180
	$\tilde{A}^2\Pi_u$	2	3	2	4		1.228	180
	$\tilde{B}^2\Sigma_u^+$	2	4	1	4		1.180	180
CS_2^+	$\tilde{X}^2\Pi_g$	2	4	2	3		1.554	180
	$\tilde{B}^2\Sigma_u^+$	2	4	1	4		1.564	180
CO_2	$\tilde{X}^1\Sigma_g^+$	2	4	2	4		1.162	180
	$\tilde{A}^1B_2$	2	4	2	2 1	1	1.246	122
CS_2	$\tilde{X}^1\Sigma_g^+$	2	4	2	4		1.554	180
	$\tilde{a}^3A_2$	2	4	2	1 2	1	1.64	136
NO_2	$\tilde{X}^2A_1$	2	4	2	2 2	1	1.19	134
	$\tilde{C}^2B_2$	2	4	2	2 1	2	1.31	121
SO_2	$\tilde{X}^1A_1$	2	4	2	2 2	2	1.43	120
	$\tilde{a}^3B_1$	2	4	2	2 2	1 1	1.494	126
	$^1A_2$	2	4	2	2 1	2 1	1.53	99
	$^1B_2$	2	4	2	1 2	2 1	1.56	104
CF_2	$\tilde{X}^1A_1$	2	4	2	2 2	2	1.300	105
	$\tilde{A}^1B_1$	2	4	2	2 2	1 1	1.32	122
ClO_2	$\tilde{X}^2B_1$	2	4	2	2 2	2 1	1.473	118
	$^2A_2$	2	4	2	1 2	2 2	1.619	107

One feature of all three groups of molecules is that in each there is one molecular orbital the occupation of which has a profound influence on the valence angle. In the HAB group this is the sixth valence molecular orbital $a's_A-\pi^*$. Thus in the ground state of HCN (a molecule with 10 valence electrons) this orbital is empty, and the molecule is linear. Promotion of one electron to the $a's_A$ orbital leads to a strongly bent $^1A''$ excited state. The HCO radical has one electron in this orbital in its ground state, and is bent. Promotion of this electron to $a''-\pi^*$ results in a linear excited state. HNO has two electrons in $a's_A$; it has a very bent ground state, but this bond angle increases in the excited electronic state resulting from the promotion of one of these electrons to the $a''-\pi^*$ orbital. The $a_1's_A-\pi_u^*$ molecular orbital has a similar influence on the bond angle of the AB_2 group of molecules: NO_2 is the first AB_2 molecule to have a non-linear ground state.

The molecular orbital diagrams provide a most satisfactory model for correlating bond length and bond angle changes from molecule to molecule and from state to state within these families. Nevertheless, the electronegativities of the constituent atoms have a marked effect upon the excitation energies. For example, all known 15 valence electron AB_2 or ABC molecules have a linear $^2\Pi$ ground state. For BO_2, CO_2^+ and NCS the first excited state is $^2\Pi$ also, with a higher lying $^2\Sigma^+$ state; the converse is true for NCO.

V. SPECTROSCOPY OF CONTINUUM STATES

All of our spectroscopic considerations thus far have been concerned with bound electronic states, supporting well defined

vibrational and rotational energy levels. Typically, however, a molecule will possess at least as many dissociative (repulsive) states as bound states. Most are completely uncharacterised, since absorption to these states generates broad, structureless continua which defy conventional analysis.

Photofragment Spectroscopy (Wilson, 1970) provides one solution to this problem. In this technique a molecular beam is crossed with short duration pulses of linearly polarised laser light and the distribution of the recoiling photofragments is measured (using a mass spectrometer) as a function of:

(i) the incident photon energy

(ii) the mass of the fragments

(iii) the fragment translational energy

(iv) the angle of fragment recoil relative to the electric vector of the photolysis laser radiation.

From such measurements it is possible to derive information about the transition moment direction and thus the (dissociative) excited state symmetry, as well as information about the fragments and their internal energy state population distributions, molecular bond strengths and the photofragmentation dynamics.

The use of linearly polarised light results in the selective excitation of those parent molecules for which the product $\underset{\sim}{\mu}.\underset{\sim}{\varepsilon}$ is a maximum, i.e.those molecules for which the transition moment lies parallel to the $\underset{\sim}{\varepsilon}$-vector. Consider, as the simplest illustrative example, the photofragmentation of a diatomic molecule. It must dissociate along its internuclear axis; the relative momentum of the recoiling atoms will thus be directed either parallel ($\Delta\Lambda=0$) or perpendicular ($\Delta\Lambda=\pm1$) to the transition moment. In either instance the resulting atomic photoproducts will show an anisotropic angular

distribution which, in the centre of mass coordinate system, takes the form:

$$I(\theta) = \frac{1}{4\pi}\left[1 + 2\beta P_2(\cos\theta)\right] \qquad (34)$$

where θ is the angle between the detection direction and $\underset{\sim}{\varepsilon}$, $P_2(\cos\theta)$ is the second order Legendre polynomial

$$P_2(\cos\theta) = \tfrac{1}{2}(3\cos^2\theta - 1) \qquad (35)$$

and β is the anisotropy parameter. β takes limiting values of +1.0 for $\Delta\Lambda=0$ transitions ($I(\theta)$ shows a $\cos^2\theta$ distribution) and -0.5 for $\Delta\Lambda=\pm1$ transitions ($I(\theta)$ proportional to $\sin^2\theta$). Reduced anisotropies are to be expected in the case of near threshold dissociations, and in those instances where the excited state (pre)dissociates on a timescale comparable to that of the rotational period. Cl_2 photoexcitation at 347nm accesses a structureless absorption continuum. Fig.14 reveals that the majority of the product Cl atoms recoil at an angle $\theta \sim 90^\circ$, perpendicular to the $\underset{\sim}{\varepsilon}$-vector of the light rather than near 0°, parallel to the $\underset{\sim}{\varepsilon}$-vector. This points to the $^1\Pi_u$ character of the dissociative excited electronic state. Analysis of the Cl atom time-of-flights provides additional insight into the dissociation process: their measured average translational energy indicates that both Cl atoms are formed in the ground ($^2P_{3/2}$) state.

The extension of these ideas to polyatomic molecules is relatively straightforward provided due allowance is made for the fact that, in the photofragmentation of a polyatomic, the direction of fragment recoil need not lie along an axis of symmetry. The angle χ between $\underset{\sim}{P}$ (the momentum vector of the recoiling fragments)

and $\underset{\sim}{\mu}$ may take any value (or range of values) between 0° and 90°.

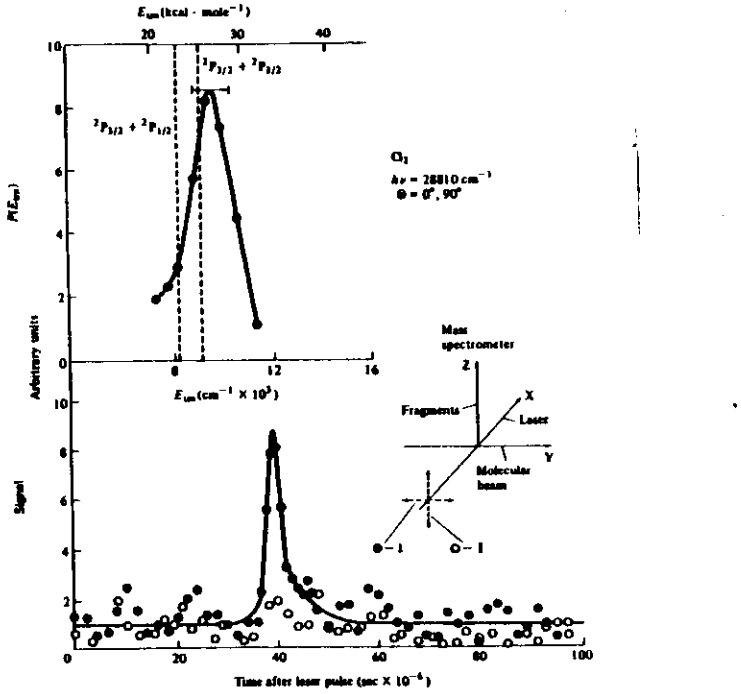

Fig.14 Cl_2 photofragment spectrum following excitation at 347nm. The lower distribution reveals that most Cl atoms recoil near $\theta=90^\circ$ (●). This implies that the upper state has $\Omega=1$. When the $\theta=90^\circ$ time of flight distribution is transformed into a distribution in total translational energy E_{trn}, the predicted energy for dissociation into ground state Cl atoms falls within the estimated uncertainty range, while that for the product channel $Cl(^2P_{3/2}) + Cl(^2P_{1/2})$ does not. Thus, measurements of the direction of recoil and of translational energy are both consistent with the assignment of $^1\Pi_{1u}$ for the symmetry of the dissociative excited state.

VI. PHOTOPHYSICS AND PHOTOCHEMISTRY

Photoexcitation results in an electronically excited molecule which is no longer in equilibrium with its surroundings; its energy may relax by a variety of mechanisms, including:

(i) re-emission as fluorescence

(ii) re-emission as phosphorescence (being spin-forbidden this is a much slower radiative decay process than (i)).

(iii) degradation to vibrational energy and thence to heat.

(iv) photochemical decomposition.

(v) energy transfer to another molecule.

(vi) chemical reaction.

Which process (or processes) occur depends not only on the molecule and on the particular quantum state excited, but also upon the environment in which the molecule finds itself. Several of these relaxation processes require intermolecular interactions, both to provide a coupling between different molecular degrees of freedom and to conserve overall energy. Excited electronic states which can relax via an allowed radiative decay process typically have fluorescence lifetimes in the range 10^{-5}-10^{-9}s. In the gas phase the typical time between collisions is 10^{-10}s at a pressure of 1 atmosphere, or 10^{-4}s at 1mTorr. Excited state relaxation in the gas phase is thus 'collision free' only at low pressures; in liquids, solvent interactions play a dominant role.

VI.1 Diatomic Molecules

I_2 fluorescence exhibits behaviour typical of diatomic molecules. Monochromatic excitation in the gas phase at low pressures

leads to resonance fluorescence from each excited v',J' level; each v' - v" band in the emission spectrum consists of a single P line and a single R line. Increased I_2 pressure, or the addition of foreign gas, causes energy transfer by collisions between excited I_2 levels, so that the wavelength resolved fluorescence spectrum now includes transitions from excited state levels other than the initially populated v',J' level. Fig.15 shows such a spectrum at a resolution which demonstrates vibrational energy transfer.

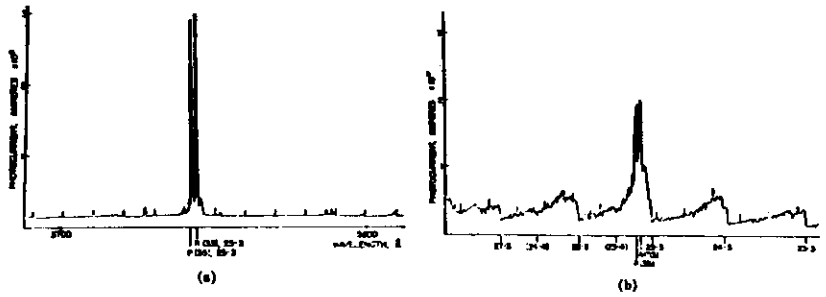

Fig.15 Fluorescence from I_2 vapour at 298K: (a) 0.2Torr I_2, (b) 0.2Torr I_2 in the presence of 3.1Torr H_2. Excitation at 546.1nm prepares the v'=25,J'=34 level of the $B^3\Pi^+_{0u}$ state from which in (a) resonance fluorescence is observed. In (b) many other emitting vibrational levels of the B state are produced by collision with H_2 (after J. Chem. Phys. 42, 3475, (1965))

Three basic types of inelastic transition can occur:

(a) change in rotational state

(b) change in vibrational state

(c) change in electronic state.

The energy level separations generally increase in the order (a)<(b)<(c), as does the strength of the interaction needed to bring about the inelastic transition. Thus the efficiencies of the various processes decrease in the order (a)>(b)>(c). In the case of I_2

therefore, increase in pressure leads to the following sequence of changes in the wavelength resolved fluorescence spectrum:

(i) resonance fluorescence from the initially populated v',J' level,

(ii) rotational energy transfer to other J' levels within the v' state,

(iii) vibrational and rotational energy transfer within the excited electronic state, and

(iv) complete loss of fluorescence (quenching) as a result of electronic energy transfer to high levels of the ground electronic state.

Not all excited state levels fluoresce at very low pressures even when they possess a favourable radiative transition probability and an apparently sharp absorption spectrum. Predissociation may result in photochemical decomposition of the excited state at a rate which is fast in comparison with radiative decay (fluorescence). Fig.16 shows that in the emission spectrum of AlH referred to in section II.4 the (1,0) band consists only of those lines for which J'<8. Above this the rotational structure breaks off abruptly, though rotational lines involving higher J' levels are known in absorption. In this case the relaxation process is:

$$AlH\ (^1\Pi) \longrightarrow Al\ (^2P) + H\ (^2S) \qquad (36)$$

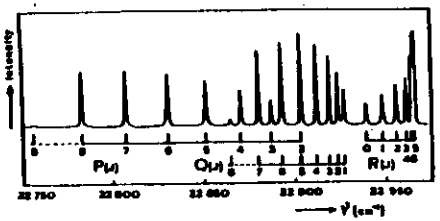

Fig.16 Breaking off in the rotational structure of the 435.3nm emission band of AlH. The last lines in the three branches are R(6), Q(7) and P(8), each of which originate from J'=7.

In this case detailed analysis has shown that the potential function U(R) possesses a maximum between the bound well of the $^1\Pi$ state and the dissociation asymptote. Predissociation then occurs by tunnelling through this barrier from the higher quasi-bound rotational levels in the well to the continuum.

Predissociation can also occur as aresult of curve crossing. Fig.17 illustrates a situation where the potential curves of a bound and of a dissociative state interact weakly resulting in an avoided crossing. In such a case the Born-Oppenheimer separation is no longer valid, since Ψ_e will depend sensitively on R in the region of the avoided crossing. However, with a weak interaction the pattern of excited state levels will approximate to those of the deperturbed state (2), with predissociation rates determined by the crossing from state (2) to state (3) - controlled in part by the Franck-Condon principle.

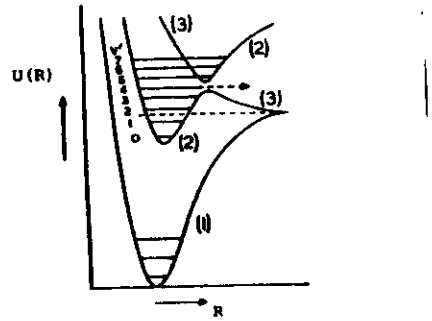

Fig.17 Predissociation of the levels of a bound electronic state (2) by the perturbing effect of a repulsive state (3)

VI.2 Polyatomic Molecules

Large polyatomic molecules have many vibrational degrees of freedom, and consequently a much larger density of vibrational states than a diatomic molecule. To a first approximation the number of vibrational states in a harmonic oscillator with n modes up to energy E_v above the zero point level is given by:

$$N(E_v) = \frac{(n + \bar{v})!}{n!\bar{v}!} \qquad (37)$$

where the mean number of vibrational quanta $\bar{v}$ is related to the geometric mean frequency $\bar{\omega}$ by:

$$v = \frac{E_v}{h\bar{\omega}} \qquad (38)$$

This simple model predicts the following density of vibrational states associated with high levels of the electronic ground state at an energy $30000cm^{-1}$ above the zero-point level:

(a) H_2CO: n=6, $\bar{\omega} \sim 1750cm^{-1}$, v=17, $g(E) \approx 17/cm^{-1}$

(b) C_6H_6: n=30, $\bar{\omega} \sim 1200cm^{-1}$, v=25, $g(E) \approx 2 \times 10^{12}/cm^{-1}$

where $g(E) = dN(E)/dE$. Thus, whereas the relaxation of electronically excited I_2 is dominated by resonant processes, that of benzene tends to be statistical. Molecules of the size of formaldehyde are intermediate, the upper levels of the ground state forming a 'lumpy' continuum at the energy of excited electronic states.

Figs.18 and 19 depict, respectively, the radiative and non-radiative processes in the form of a Jablonski diagram. Even molecules of the size of benzene are capable of giving resonance fluorescence if excited at sufficiently low pressures. However, at

pressures in excess of about 1 Torr, or in condensed phases, the fluorescence is independent of the frequency of the exciting radiation as a result of rapid vibrational relaxation within the excited electronic state. This relaxation, and its consequences in terms of Franck-Condon factors, has important implications for the efficiency of dye lasers.

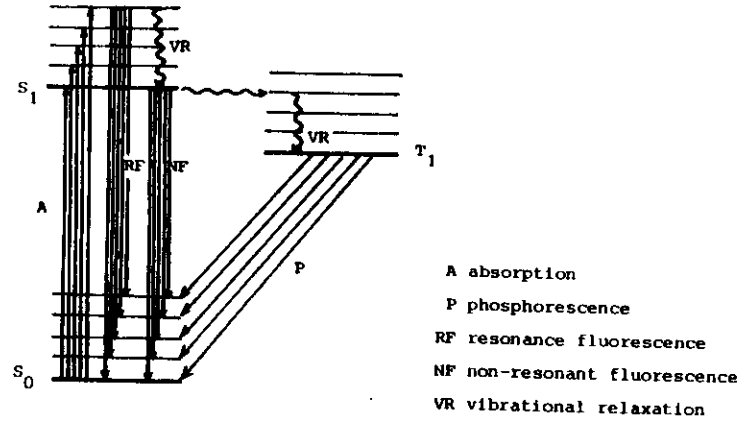

Fig.18 Jablonski diagram depicting the important radiative processes in a typical organic molecule.

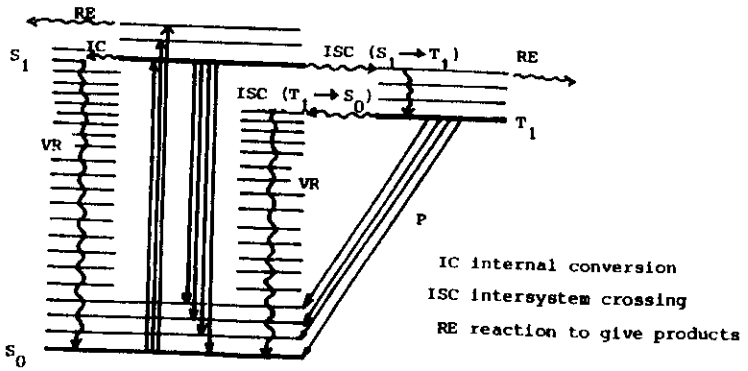

Fig.19 State diagram showing the important electronic and vibrational relaxation processes in competition with emission.

Excited triplet states have longer radiative lifetimes than the corresponding singlet states since their phosphorescence violates the $\Delta S=0$ selection rule. Thus triplet state emissions are more easily quenched by both physical and reactive mechanisms. Even so, small molecules like SO_2 and H_2CO do give triplet $\longrightarrow$ singlet emissions at very low pressures. Many aromatic molecules also phosphoresce when in dilute solution or in rigid glasses, the excited triplet state having been populated by intersystem crossing from an excited singlet state.

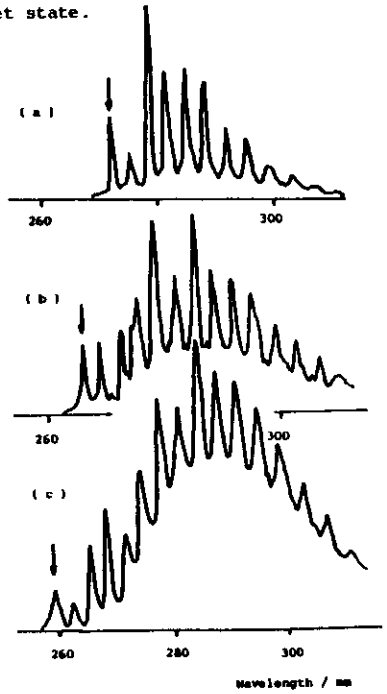

Fig.20 Resonance fluorescence from "isolated" p-difluoro-benzene excited at different wavelengths (arrowed) corresponding to (a) zero-point level, (b) one and (c) two quanta of ν_1 (totally symmetric C—C breathing mode) respectively. (adapted from J. Photochem. 3, 365, (1974/5)).

Acknowledgement

It is a pleasure to acknowledge the considerable assistance provided by Professor R.N.Dixon in the preparation of these lecture notes.

References

J.H.Callomon, T.M.Dunn and I.M.Mills, Phil. Trans. Roy, Soc., A259, 499, (1966)

G.H.Dieke and G.B.Kistiakowsky, Phys. Rev. 45, 4, (1934)

R.N.Dixon, "Spectroscopy and Structure", Methuen, London, (1965)

G.Duxbury in "Molecular Spectroscopy" (Chem. Soc. Spec. Per. Report) 3, 497, (1975)

A.G.Gaydon, "The Spectroscopy of Flames", Chapman and Hall, London, (1974)

G.Herzberg, "Molecular Spectra and Molecular Structure.I. Spectra of Diatomic Molecules", Van Nostrand Reinhold, New York, (1950)

G.Herzberg, "Molecular Spectra and Molecular Structure.III. Electronic Spectra and Electronic Structure of Polyatomic Molecules", Van Nostrand Reinhold, New York, (1966)

C.K.Ingold and G.W.King, J. Chem. Soc., 2702, (1953)

A.J.Merer and R.S.Mulliken, Chem. Rev., 69, 639, (1969)

R.S.Mulliken, Acc. Chem. Res., 9, 7, (1976)

J.I.Steinfeld, "Molecules and Radiation", M.I.T.Press, Cambridge, Mass., (1974)

A.D.Walsh, J. Chem. Soc., 2260, 2266, 2290, (1953)